An Accurate Quantum Monte Carlo Calculation of the Barrier Height for the Reaction $H + H_2 \rightarrow H_2 + H$

Drake L. Diedrich and James B. Anderson

An improved quantum Monte Carlo method has been used to calculate the classical barrier height for the hydrogen exchange reaction $H + H_2 \rightarrow H_2 + H$ with accuracies greater than previously attained. The method is exact in that, except for the easily estimated Monte Carlo statistical or sampling error, it requires no mathematical approximations or physical approximations beyond those of the Schrödinger equation. The minimum in the barrier, occurring for the collinear nuclear configuration with the protons separated by 1.757 bohrs, was found to be 9.61 ± 0.01 kilocalories per mole above $H + H_2$.

The reaction $H + H_2 \rightarrow H_2 + H$ and its isotopic variants are the only reactions for which accurate three-dimensional quantum scattering calculations have been made with a potential energy surface accurate to within about 1 kcal/mol. After several iterations back and forth between experiment and theory there is now excellent agreement for many experimentally measured and theoretically predicted reaction characteristics (*1*, *2*), but the agreement is not complete and there remain significant differences between experiment and theory for several characteristics. In particular, for the reaction $D + H_2(v = 1, j = 1) \rightarrow HD(v' = 1, j') + H$, where v and j are, respectively, vibrational and rotational quantum numbers, the calculated rotational energy is higher than that measured and the calculated enhancement of the rate of production of $v' = 1$ with increasing v is higher than that measured (*2*, *3*). Also, the measured time-of-flight distributions of reaction products in crossed-beam reactions of D with H_2 (*4*) are not in agreement with theoretical predictions (*5*, *6*). The failure to obtain complete quantitative agreement may be due to inaccuracies in the potential energy surface used for predictions, to a possible defect in the quantum scattering calculations, or to unknown artifacts in the experiments.

The most accurate quantum scattering calculations have been carried out with either of two potential energy surfaces obtained from analytic fits to energies calculated for a large number of nuclear configurations. The LSTH surface (*6*) obtained with points from variational calculations by Liu (*7*) and by Siegbahn and Liu (*8*) has a barrier height of 9.80 kcal/mol relative to separated $H + H_2$. The DMBE surface (*9*) obtained with points from several calculations and adjusted to fit the barrier height given in earlier quantum Monte Carlo calculations (*10*) has a barrier height of 9.65 kcal/mol. A recently proposed BKMP surface (*11*) based on more points from variational calculations has a barrier height of 9.54 kcal/mol.

The lowest energy analytic variational calculations to date are those of Liu (*12*), which yield a minimum in the barrier height of 9.86 kcal/mol relative to the exact value for separated $H + H_2$ and 9.65 kcal/mol relative to the value for $H + H_2$ calculated with the same basis set. From these values, Liu estimated the true value of the minimum in the barrier to be 9.53 to 9.65 kcal/mol. The saddle point configuration was collinear with a separation of 1.757 bohrs between neighboring protons. For the same configuration, quantum Monte Carlo calculations with released nodes carried out by Ceperley and Alder (*10*) gave a barrier height of 9.65 ± 0.08 kcal/mol relative to $H + H_2$.

In our calculations for the H-H-H system we used an exact quantum Monte Carlo method (*13*) for many-electron systems, which is based on the partial cancellation of positive and negative wave function samples that have overlapping Green's functions. The method combines many of the best features of fixed-node (*14*), released-node (*10*), and cancellation methods (*15*) with sample relocation after node crossing, self-cancellations, multiple cancellations, and maximum use of symmetry in promoting cancellations. With this method it has been possible to achieve a stable population of samples with a large ratio of positive to negative samples. The energy of the system is obtained from these samples with the aid of an importance sampling function (*16*) in the form of an approximate wave function for the system.

The Green's function quantum Monte Carlo method (*17*) provides solutions to the time-independent Schrödinger equation:

$$-\frac{\hbar^2}{2m}\nabla^2\Psi(X) + V(X)\Psi(X) = E\Psi(X) \quad (1)$$

where $\hbar$ is Planck's constant divided by 2π, m is the mass of the electron, V is the electrostatic potential energy, and E is the energy. The solutions are obtained in the form of samples of the exact wave function $\Psi(X)$. Sampling is based on the property of the Green's function $G_0(X,X')$, which relates the wave function to itself:

$$\Psi(X) = \int G_0(X,X')\frac{V(X')}{E}\Psi(X')dX' \quad (2)$$

Repeated application of Eq. 2 to an initially arbitrary wave function $\Psi(X')$ leads to a wave function $\Psi(X)$, which is the lowest energy solution to the Schrödinger equation for the specified boundary conditions or other constraints. The theoretical basis for cancellation of positive and negative samples is described in (*13*, *15*). In the absence of cancellation, the wave function would be given by the small difference between large populations of positive and negative samples. With cancellation, a stable, net positive population is easily maintained.

The estimate of the energy obtained from Monte Carlo sampling is given by a weighted average of local energies $E_{loc} = H\Psi_T/\Psi_T$, where H is the Hamiltonian, for a trial wave function Ψ_T used in importance sampling,

$$E = \frac{\Sigma s_i W_i \Psi_T E_{loc}}{\Sigma s_i W_i \Psi_T} \quad (3)$$

where s_i is the sign of a sample (Ψ-based) and W_i is its weight. The use of importance sampling reduces the uncertainty in the energy but does not affect the (average) value of the energy. The uncertainty in the energy depends on the accuracy of the trial function and the number of samples. It is directly proportional to the standard deviation σ_i in local energy and inversely proportional to the square root of the number of samples. Thus, an accurate trial function or a large number of samples, or both, are desired.

The trial function for importance sampling was a simple product function of the type we have used previously, modified with a Jastrow function incorporating terms suggested by others (*18*). We optimized the function by adjusting coefficients to minimize the variance in local energies for a large number of samples. The standard deviations in local energies from the exact values ranged from 0.3 to 0.4 hartree for the nuclear configurations investigated.

The input energies E for multiplying by V/E in Eq. 2 were obtained in preliminary runs. We tested the effect of any error in

Department of Chemistry, Pennsylvania State University, University Park, PA 16802.

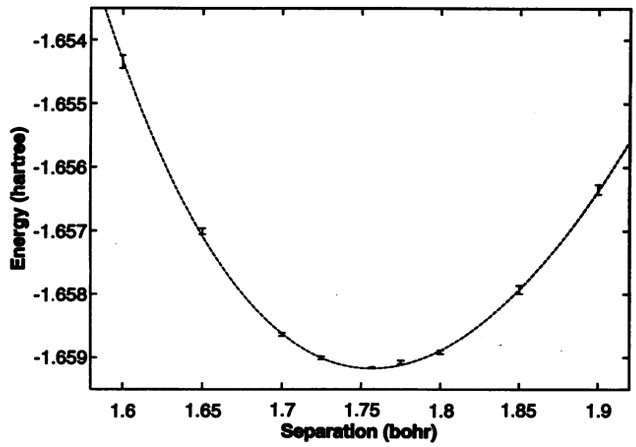

Fig. 1 (left). Electronic energies calculated for collinear symmetric H-H-H.

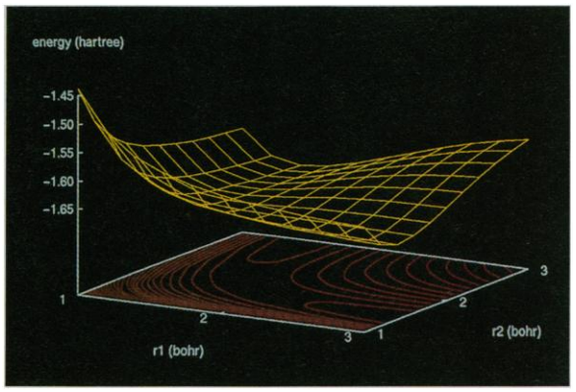

Fig. 2 (right). The potential energy surface for collinear H-H-H.

Table 1. Calculated energies for H-H-H; a_0 = Bohr radius.

Configuration R_1, R_2, Θ (a_0, a_0, deg)	Energy E (hartrees)	Energy* $E - E_{H + H_2}$ (kcal/mol)
	Collinear	
$R_1 = R_2 = 1.600$	−1.654415 (118)	12.59 ± 0.07
1.650	−1.657007 (046)	10.96 ± 0.03
1.700	−1.658636 (024)	9.94 ± 0.02
1.725	−1.659004 (026)	9.71 ± 0.02
1.757	−1.659154 (014)	9.61 ± 0.01
1.775	−1.659072 (027)	9.67 ± 0.02
1.800	−1.658910 (029)	9.77 ± 0.02
1.850	−1.657927 (064)	10.38 ± 0.04
1.900	−1.656343 (078)	11.38 ± 0.05
	H + H_2	
$R_1 = 20.0$, $R_2 = 1.401$	−1.674451 (023)	0.02 ± 0.02
$R_1 = \infty$, $R_2 = 1.4025$ (*19*)	−1.674476	0.0

*Energy relative to that for separated H + H_2, having a clamped-nucleus energy of −1.674476 hartrees, as determined by interpolation of results of analytic variational calculations by Kolos *et al.* (*19*).

the input energy on the output energy by introducing large errors in the input energy. An input error of 200 kcal/mol led to an output error of only about 0.5 kcal/mol. Thus, the actual input errors of less than 0.1 kcal/mol led to negligible output errors.

We carried out the calculations on IBM RS/6000-550 and -320H workstations by using 18 to 283 independent runs for each nuclear configuration. The uncertainties in the average energies were determined from the variances in the energies for individual runs. The total computation time for the most accurate calculation, that of the saddle point, was about 80 machine-days. For the less accurate calculations of other configurations, the total times were only 4 machine-days.

The results are listed in Table 1 and plotted in Fig. 1. The minimum energy calculated for collinear configurations with $R_1 = R_2$ (R_1 and R_2 are the distances between atoms) was that for $R_1 = R_2 = 1.757$ bohrs, which is −1.659154 ± 0.000014 hartrees and corresponds to 9.61 ± 0.01 kcal/mol relative to exact H + H_2. The indicated uncertainty is 1 SD. A least squares fit of the data to a fourth-order polynomial in R produced a curve with a minimum at $R = 1.757$ bohrs with an energy of −1.659157 hartrees, 9.61 kcal/mol above H + H_2.

To test our program and procedures, we also made a calculation for collinear separated H + H_2 using the same trial function for importance sampling as in the barrier region. This gave an inefficient calculation but a better test. For the internuclear distances of $R_1 = 20.0$ bohrs and $R_2 = 1.401$ bohrs, the calculated energy was −1.674451 ± 0.000023 hartrees. This value is in good agreement with a value of −1.174476 hartrees for H_2 with an equilibrium internuclear distance of 1.4025 bohrs, interpolated from the results of analytic variational calculations by Kolos, Szalewicz, and Monkhorst (*19*), together with the value of −0.500000 hartree for the clamped-nucleus hydrogen atom.

A comparison with the lowest energy variational calculations by Liu (*12*) for collinear configurations with $R_1 = R_2$ equal to 1.70, 1.75, and 1.80 bohrs shows that our calculated energies are 0.25 to 0.28 kcal/mol less. Liu's curve and our curve are identical in shape within our uncertainty in this range. Liu's estimate of 9.59 ± 0.06 kcal/mol is in agreement with our value of 9.61 ± 0.01 kcal/mol for the minimum in the barrier. The earlier quantum Monte Carlo value of 9.65 ± 0.08 kcal/mol (*10*) is also in agreement with our value.

The accuracy of our Monte Carlo calculations for the H-H-H saddle point configuration is 0.000014 hartree or 3 cm^{-1}. Clementi *et al.* (*20*) recently speculated that an analytic variational calculation for H-H-H accurate to within 10 cm^{-1} of the exact value "would call for somewhere around 3500 years" on a computer similar to the ones we used. There are, of course, opportunities for significant improvements and reductions in computation requirements for analytic variational calculations on this system, and it may be possible to "reduce the task to 10 to 20 years" or even less (*20*). There are also opportunities for significant improvements and reductions in computation requirements for quantum Monte Carlo calculations.

We have determined additional points on the potential energy surface with accuracies of about 0.1 kcal/mol. These are plotted in Fig. 2 for the collinear configuration with R_1 and R_2 in the range of 1.0 to 3.0 bohrs. Points in other regions, for collinear and for bent configurations, can be determined with similar accuracies. Because an increase in uncertainty by a factor of 10 from 0.01 to 0.10 kcal/mol reduces the computation effort by a factor of 100, thousands of points can be determined to accuracies within 0.10 kcal/mol of their exact values.

REFERENCES AND NOTES

1. For recent reviews, see: W. H. Miller, *Annu. Rev. Phys. Chem.* **41**, 245 (1990); *Chem. Eng. News* **68** (no. 23), 32 (1990).
2. D. A. V. Kliner, D. E. Adelman, R. N. Zare, *J. Chem. Phys.* **95**, 1648 (1991).
3. N. C. Blais, M. Zhao, D. G. Truhlar, D. W. Schwenke, D. J. Kouri, *Chem. Phys. Lett.* **166**, 11 (1990).
4. S. A. Buntin, C. F. Giese, W. R. Gentry, *ibid.* **168**, 513 (1990); R. E. Continetti, B. A. Balko, Y. T. Lee, *J. Chem. Phys.* **93**, 5719 (1990).
5. J. Z. H. Zhang and W. H. Miller, *J. Chem. Phys.* **91**, 1528 (1989); M. Zhao, D. G. Truhlar, D. W. Schwenke, D. J. Kouri, *J. Phys. Chem.* **94**, 7074 (1990).
6. D. G. Truhlar and C. J. Horowitz, *J. Chem. Phys.* **68**, 2466 (1978).
7. B. Liu, *ibid.* **58**, 1925 (1973).
8. P. Siegbahn and B. Liu, *ibid.* **68**, 1074 (1978).
9. A. J. C. Varandas, F. B. Brown, C. A. Mead, D. G. Truhlar, N. C. Blais, *ibid* **86**, 6258 (1987).
10. D. M. Ceperley and B. J. Alder, *ibid.* **81**, 5833 (1984).
11. A. I. Boothroyd, W. J. Keogh, P. G Martin, M. R. Peterson, *ibid.* **95**, 4343 (1991).
12. B. Liu, *ibid.* **80**, 581 (1984).
13. J. B. Anderson, C. A. Traynor, B. M. Boghosian, *ibid.* **95**, 7418 (1991).
14. J. B. Anderson, *ibid.* **63**, 1499 (1975).
15. D. M. Arnow, M. H. Kalos, M. A. Lee, K. E. Schmidt, *ibid.* **77**, 5562 (1982).
16. R. C. Grimm and R. G. Storer, *J. Comput. Phys* **7**, 134 (1971).
17. M. H. Kalos, *Phys. Rev. A* **128**, 1791 (1962).
18 R. N. Barnett, P J. Reynolds, W A. Lester, *J. Chem. Phys* **84**, 4992 (1986); C. J. Umrigar, K. G. Wilson, J. W. Wilkins, *Phys. Rev. Lett.* **60**, 1719 (1988), K. E. Schmidt and J. W. Moskowitz, *J Chem. Phys.* **93**, 4172 (1990).
19. W. Kolos, K. Szalewicz, H. Monkhorst, *J. Chem. Phys.* **84**, 3278 (1986).
20. E. Clementi *et al.*, *Chem. Rev.* **91**, 679 (1991).

21. This work was supported by grants from the National Science Foundation (CHE-8714613) and the Office of Naval Research (N00014-92-J-1340).

18 March 1992; accepted 10 August 1992

Infrared Reflection-Absorption Spectroscopy and STM Studies of Model Silica-Supported Copper Catalysts

Xueping Xu, Scott M. Vesecky, D. Wayne Goodman

The structure of model silica-supported copper catalysts has been investigated with scanning tunneling microscopy (STM) and infrared reflection-absorption spectroscopy (IRAS). The IRAS studies of CO on the model silica-supported copper catalysts indicate that there are several types of copper clusters with surface structures similar to (111), (110), and other high-index planes of single-crystal copper. The STM studies show several types of copper clusters on silica and reveal images of metal clusters on an amorphous oxide support with atomic resolution.

The activity and selectivity of many metal-catalyzed reactions often are sensitive to the metal particle morphology (*1*). However, there are no direct techniques to determine the surface structure of supported metal catalysts with atomic resolution. Scanning and transmission electron microscopies (SEM and TEM) are widely used to examine catalysts, but SEM does not have sufficient resolution for atomic imaging, whereas TEM requires thin samples and only yields a projected image (*2*). Infrared absorption spectroscopy (IRAS) is also often used to characterize adsorbed species in situ, and the structure of the metal surface in certain cases can be inferred when the characteristic frequencies of an adsorbate on different crystal faces are available (*3*).

Scanning tunneling and atomic force microscopies (STM and AFM) are powerful techniques that directly probe the surface with atomic resolution (*4*). Although STM has successfully imaged metal and semiconductor single-crystal surfaces and epitaxially grown metal films, atomically resolved images of metal particles supported on an amorphous oxide surface have yet to be reported. Typical catalyst support materials consist of amorphous oxides. Low-resolution STM images of an oxide-supported metal catalyst have been obtained (*5*).

We report atomically resolved STM images of a model silica-supported copper (Cu/SiO_2) catalyst that include atomic-level images for metal particles on an amorphous substrate. Complementary IRAS studies of CO on the Cu/SiO_2 are also presented (*6–8*).

The SiO_2 films, whose preparation on Mo(110) has been reported previously (*9*), were characterized with Auger electron, x-ray photoelectron, electron energy loss, IRAS, and thermal programmed desorption (TPD) spectroscopies (*9, 10*). The films (~100 Å thick) are thermally stable up to 1600 K, exhibit properties of vitreous SiO_2, and have been shown to be valid models for the SiO_2 surface (*9, 10*). The SiO_2 films grow initially in a layer-by-layer fashion for the first few layers, fully covering the Mo(110) substrate (*9, 10*). The coverage of Cu (θ_{Cu}) in all cases reported here was determined with TPD (*7*). After evaporative deposition, the Cu films were annealed to 700 K and cooled to 300 K before being transferred to air for STM and AFM studies.

A series of IRAS spectra of CO chemisorbed on several Cu/SiO_2 catalysts is shown in Fig. 1. The Cu was deposited onto the SiO_2 thin film at 100 K, annealed to 900 K, cooled to 90 K, and then saturated with CO. At low θ_{Cu} [<0.3 monolayer (ML)], two IR bands are apparent at 2110 and 2062 cm^{-1}. As θ_{Cu} was increased from 1.1 to 3.4 ML, a new IR band appeared at 2094 cm^{-1}, and the band at 2062 cm^{-1} shifted to 2074 cm^{-1}. At 15 ML of Cu, a prominent band was observed at 2102 cm^{-1}, with two shoulders at 2087 and 2070 cm^{-1}. Upon heating to 900 K, evaporated Cu forms three-dimensional (3-D) clusters on SiO_2 with a dispersion of ~0.4 at an effective θ_{Cu} of 2 ML (*8*). These IR bands can then be assigned to specific CO adsorption sites directly related to distinct morphologies of the 3-D Cu clusters.

Adsorption of CO on Cu single-crystal surfaces has been extensively studied by IRAS. Adsorption on low-index Cu planes

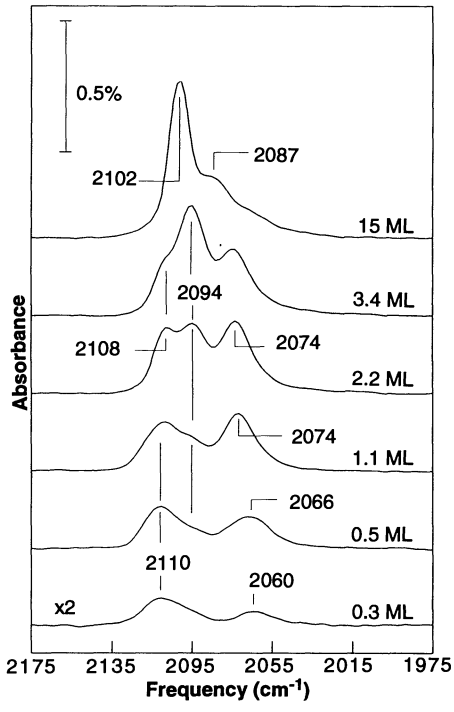

Fig. 1. Infrared reflection-absorption spectra of CO on copper/silica (100 Å)/Mo(110). Copper was deposited at 90 K and annealed to 900 K. The Cu coverages are 0.3, 0.5, 1.1, 2.2, 3.4, and 15 monolayers, respectively (ML; 1 ML = 1.3×10^{15} atom/cm^2). Carbon monoxide was adsorbed at 90 K to saturation.

Department of Chemistry, Texas A&M University, College Station, TX 77843–3255.